International Journal of Biological Macromolecules 302 (2025) 140519

Contents lists available at ScienceDirect

International Journal of Biological Macromolecules

journal homepage: www.elsevier.com/locate/ijbiomac

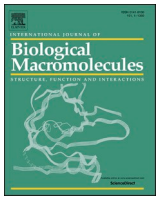

Bioactive lignin from maleic acid hydrotropic fractionation: Revealing the structural–bioactivity relationship

Chen Su [a,b,c,d], Xiu Wang [b,c], Kolby Hirth [d], Matthew Arvanitis [d], Yunfeng Cao [c], Guigan Fang [a,b,c], J.Y. Zhu [d,*]

[a] Institute of Chemical Industry of Forest Products, Chinese Academy of Forestry, Nanjing 210042, China
[b] Key Lab. of Biomass Energy and Material, Jiangsu Province, Nanjing 210042, China
[c] Jiangsu Co-innovation Center for Efficient Processing and Utilization of Forest Resources, Jiangsu Provincial Key Lab Pulp & Paper Science and Technology, Nanjing Forestry University, Nanjing 210037, China
[d] USDA Forest Products Laboratory, Madison, WI 53726, United States

ARTICLE INFO

Keywords:
Lignin
Physicochemical structures
Maleic acid hydrotropic fractionation
Antioxidant
Antibacterial
UV-blocking

ABSTRACT

Lignin possesses diverse bioactivities due to its unique physicochemical structure. This study investigates the structural-bioactivity relationships of lignin derived from maleic acid hydrotropic fractionation (MAHF) of two types of herbaceous biomass. The results indicated that lignin with higher phenolic hydroxyl (-OH) content (up to 2.0 mmol/g) and carboxyl (-COOH) groups (up to 0.89 mmol/g) exhibited significantly enhanced antioxidant activity. The highest antioxidant of MAHF lignin (MAHL) reached 98 % for scavenging DPPH (2,2-diphenyl-1-(2,4,6-trinitrophenyl)hydrazyl) at 0.56 mg/mL. Antibacterial tests revealed that MAHLs demonstrated inhibition rates of 66 % against *E. coli* and 54 % against *S. aureus* at 10 mg/mL. MAHLs at 1 mg/mL concentration blocked >98 % of UV radiation. Furthermore, the study demonstrated that lignin with higher phenolic hydroxyl (-OH), carboxyl (-COOH), and syringyl (S) units and conjugated double bonds exhibit enhanced bioactive properties. Lignin with lower Mw and PDI also tends to possess good bioactivities. The findings from the study can facilitate the application of lignin as an efficient, cost-effective, and renewable biopolymer additive in various industries.

1. Introduction

Petroleum-based or chemical synthetic materials are expected to be replaced by materials derived from natural resources to reduce the human carbon footprint [1–3]. Biobased materials possess multifunctional features, including antioxidant, antibacterial, and ultraviolet (UV) blocking properties, which are highly sought after by many industries such as food packaging, medical supplies, textiles, and clothing [4,5]. Lignin, the second most abundant biopolymer from plant biomass is biologically active due to its diverse supermolecular structure and various functional groups [6,7]. Utilizing the bioactivity of lignin for developing new green bioactive materials can facilitate high-value biomass utilization for a low-carbon economy [8,9].

The bioactivities of lignin are related to its structural properties. Lignin with high phenolic hydroxyl (-OH) content, low weight-averaged molecular weight (Mw), and narrow polydispersity index (PDI) exhibited favorable antibacterial properties [10,11]. The condensed structures (such as C—C, β-5′, and β-β' bonds) and double-bond structures (such as -COOH groups) in lignin were beneficial to UV-blocking activity [12,13]. Furthermore, the unsaturated groups or benzene rings in lignin can also enhance UV-blocking activity [14]. Lignin with low Mw and high phenolic -OH or -COOH contents showed prominent antioxidant properties [15,16]. Although progress has been made in elucidating the relationship between lignin structures and bioactivities, deficiencies remain. For example, only the relation between single bioactivity and lignin physicochemical structures has been studied so far, and the relationships between lignin triple bioactivities and its physicochemical characteristics are not well understood. Moreover, most lignin samples used in earlier studies [12,13] have low and small variations in -COOH and phenolic -OH contents, which made assessment of the effects of these two properties on lignin bioactivities difficult.

Both the lignin physical properties such as Mw and PDI and chemical structures such as phenolic -OH, -COOH, C—C, β-5′, and β-β' bonds could affect its bioactivities [17,18]. Fractionation of lignin with diverse structures from plant biomass can help to investigate the relation between structures and bioactivities. Conventional wood pulping

* Corresponding author.
E-mail address: junyong.zhu@usda.gov (J.Y. Zhu).

https://doi.org/10.1016/j.ijbiomac.2025.140519
Received 10 July 2024; Received in revised form 15 January 2025; Accepted 29 January 2025
Available online 30 January 2025
0141-8130/Published by Elsevier B.V.

Table 1
List of different MAHLs and their corresponding fractionation conditions and yields.

Raw material	Wheat straw			Switchgrass		
Fractionation conditions	Mild	Moderate	Severe	Mild	Moderate	Severe
	M40T80t120	M60T100t30	M60T120t30	M40T80t120	M60T100t30	M60T120t30
Lignin samples	T80-W	T100-W	T120-W	T80-S	T100-S	T120-S
Fractionation severity (CDF)	33.5	124.0	300.0	0.6	7.6	42.7
Lignin removal (%)	37.8	53.6	56.6	18.7	46.8	57.8

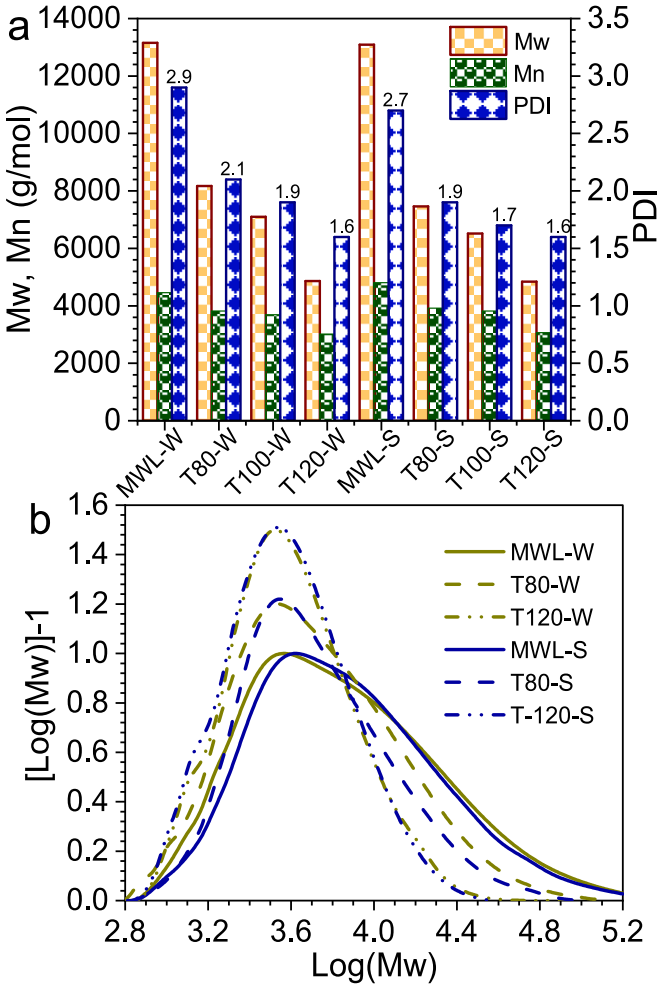

Fig. 1. (a) MAHL average molecular weights and distribution polydisperse indices (PDI); (b) MAHL molecular weight distributions.

processes tend to produce highly condensed lignin structures [19]. Maleic acid hydrotropic fractionation (MAHF) has recently emerged as a promising process to fractionate maleic acid hydrotropic lignin (MAHL) with diverse properties from biomass [20–22]. MAHL with greater phenolic -OH content, low Mw, and low PDI [23,24] is desirable for improving bioactivities. Furthermore, MAHL can be highly esterified with great amounts of C—C, β-5′, and β-β’ bonds under severe fractionation conditions [20,22–24]. Therefore, MAHF provides a means to produce lignin with a range of physicochemical structures, making it suitable for analyzing the relationship between lignin physicochemical structures and multibioactivities [22,25]. Moreover, maleic acid is a U.S. Food and Drug Administration (FDA) approved indirect food additive (21CFR175- 177, Code of Federal Regulations (CFR)) and MAHF does not use sulfur. The resultant MAHL is not only light-colored but also inherently safe and odorless (unlike commercial kraft lignin containing

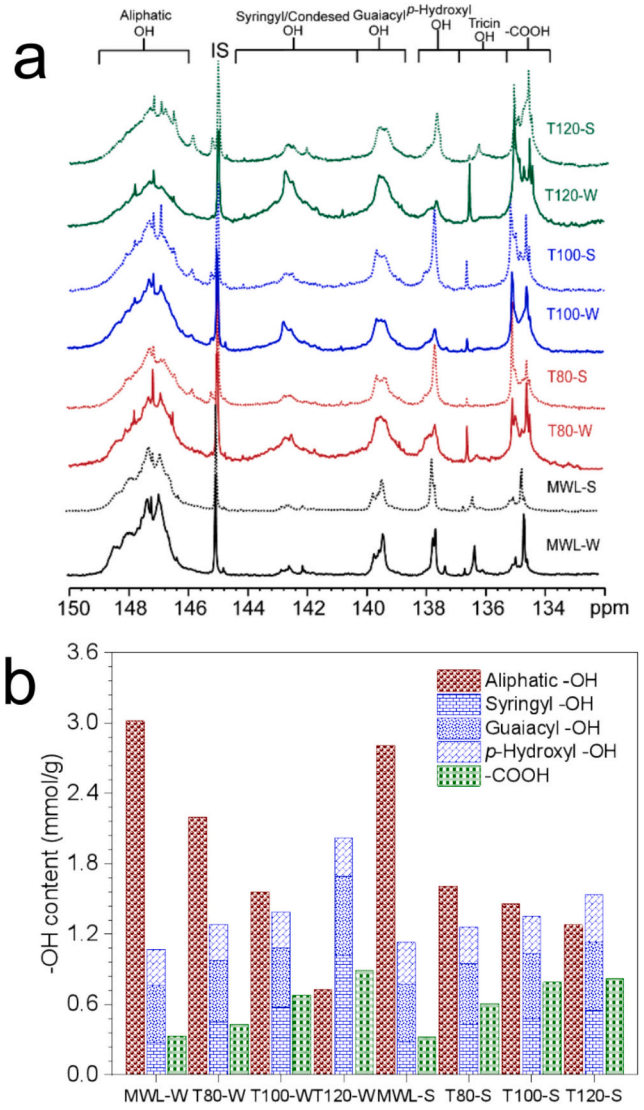

Fig. 2. (a) Quantitative ^{31}P NMR spectra of the MAHLs and MWLs; (b) Quantification of the functional groups in lignin by ^{31}P NMR spectroscopy.

sulfur), ideally suited for food, medical, and cosmetic applications [21,26].

The objective of this study is to examine the relationship between the structures of MAHL and its multibioactivities, simultaneously establishing a structure-activity relation. For meaningful comparison purposes, three sets of MAHL from different fractionation severities were selected (based on the extent of delignification or MAHF severity). The overall goal of this study is to present a fundamental understanding of the lignin structure and its bioactivity relationship for developing value-added natural biopolymers.

Table 2
Semi-quantitative amounts of lignin substructures and LCC linkages (/100 Ar) from 2D HSQC NMR spectroscopy along with the delignification of all samples.

Fractionation	MWL-W	MWL-S	M40T80t 120-W	M60T100t30-W	M60T120t30-W	M40T80t120-S	M60T100t30-S	M60T120t30-S
Lignin samples	MWL-W	MWL-S	T80W	T100W	T120W	T80S	T100S	T120S
Delignification	–	–	37.8	53.6	56.6	18.7	46.8	57.8
Lignin Purity (%)	95.4 ± 1.1	94.7 ± 0.9	95.5 ± 1.7	96.6 ± 1.0	98.1 ± 1.3	94.4 ± 2.1	97.0 ± 0.8	97.4 ± 1.6
Interunit linkages [b]								
β-O-4'	53.6	47.7	48.8	40.1	25.5	41.2	33.3	29.2
β-5'	6.2	5.5	4.0	5.3	6.0	3.5	4.8	4.9
β-β'	7.0	6.3	7.2	8.8	9.5	2.0	1.7	2.0
Condensed degree[c]	19.8	19.9	18.6	26.0	37.8	10.5	16.3	19.1
γ-esterification	12.2	10.4	14.1	28.1	35.5	17.7	40.6	44.2
HKα	–	–	–	2.6	7.0	1.7	2.3	3.6
Aromatic units [a]								
S	39	36	49	50	58	34	36	40
Cond S	–	–	1	6	10	2	3	5
G	58	61	48	46	39	63	61	57
Cond G	–	–	4	12	19	2	9	15
H	3	3	3	4	3	3	4	3
S/G ratio	0.67	0.52	1.02	1.09	1.48	0.54	0.59	0.70
p-Hydroxycinnamates [b]								
p-coumarates	6.8	9.8	4.8	4.5	2.7	14.8	18.0	17.1
ferulates	2.0	5	2.2	1.2	0.9	1.5	2.0	1.8
Flavonoids [b]								
Tricin	9.6	4.2	3.1	1.3	1.1	0.4	0.5	0.4
LCC linkages [b]								
PhGlc	6.0	3.9	3.3	1.8	1.7	1.7	1.5	1.4
BE	7.3	3.1	2.5	1.7	1.3	1.8	1.3	1.0
Total	13.6	7.0	5.8	3.5	3.0	3.5	2.8	2.4

[a] Molar percentages (H + G + S = 100).
[b] Interunit linkages, p-coumarate, ferulate, and tricin molar contents as percentages of lignin content (H+ G + S).
[c] Condensed degree, % = 100 * ($I_{B\alpha}$ + $I_{C\alpha}$) / (I_A+ $I_{B\alpha}$ + $I_{C\alpha}$), as the integral value of each signal in 2D HSQC NMR.

2. Experimental

2.1. Materials and reagents

Switchgrass and wheat straw were used as the lignin source in the present study. The switchgrass was complementarily provided by Professor Kevin Shinner at the Department of Biological Systems Engineering, University of Wisconsin-Madison. The air-dried wheat straw was from a farm in Canada. The switchgrass and wheat straw were first Wiley-milled to pass a 10-mesh screen before use. The anhydrous maleic acid (MA) in ACS reagent grade, DPPH (2,2-diphenyl-1-(2,4,6-trinitrophenyl)hydrazyl), and ABTS diammonium salt (2,2′-azinobis(3-ethylbenzothiazoline-6-sulfonic acid) ammonium salt) in ACS high-performance liquid chromatography (HPLC) grade were purchased from Sigma-Aldrich (St. Louis, Missouri, USA). The other chemical reagents (i.e., DMSO, DMSO-$_{d6}$) were analytical grade and were purchased from Macklin Biochemical Co., Ltd. (Shanghai, China). Luria-Bertani (LB) broth was provided by Hopebio Biotechnology Co, Ltd. (Qingdao, China). The cultures of bacteria used to evaluate antibacterial activity, i.e., gram-positive bacteria *Staphylococcus aureus* (*S. aureus*) and gram-negative bacteria *Escherichia coli* (*E. coli*) were purchased from the Guangdong Engineering and Technology Research and Development Center of Microbial Food Safety.

2.2. Preparation of MAHLs and milled wood lignin

Two sets of MAHL preparations each from wheat straw and switchgrass were fractionated under different severities [27], i.e., mild, moderate, and severe conditions (Table 1), with varied levels of delignification. These fractionation runs were carried out in MA concentration ranging from 40 to 60 wt%, and reaction temperature and time from 80 to 120 °C and 30 to 120 min, respectively. For convenience, these runs were designated as M*xx*T*yy*t*zz*, where *xx*, *yy*, and *zz* represent MA concentration in wt%, fractionation temperature in °C, and duration time in min, respectively. Aqueous MA solutions were prepared in glass flasks by solubilizing desired amounts of MA in deionized (DI) water. Each flask was placed on a magnetic agitator with temperature control (C-MAG HS7DS1, IKA, USA) to facilitate dissolution of MA. Under constant stirring at a designed temperature and time, 10 g of oven-dried milled switchgrass or wheat straw were added into 150 g prepared MA solution. All fractionated water-insoluble solids (WIS) were separated from the spent liquor by filtration and followed by washing with DI water until the spent liquor (with filtrate) was diluted to 10 wt%, below the MA minimal hydrotropic concentration (MHC = 25 wt%) to precipitate lignin. After centrifuging, the lignin was dialyzed in DI water for one week and then freeze-dried. The chemical compositions of all WISs were determined by the Analytical Chemistry and Microscopy Laboratory at the USDA Forest Service, Forest Products Laboratory, in Madison, Wisconsin, USA, using the traditional two-step sulfuric acid hydrolysis, as described previously [28]. The delignification yields (lignin removals) of the resultant MAHLs under different fractionation severities in terms of combined delignification factor (CDF) along with their labels are listed in Table 1. CDF was determined based on an earlier study [24], i.e., $CDF = exp\left(\alpha' \quad \frac{E'}{RT} + \beta' C\right) \bullet C \bullet t$ with $\alpha' = 33.06$ *and* 27.16, $\beta' = 0.200$ *and* $0.965\ L/mol$, $E' = 105,000$ *and* $105,000\ J/mol$ for wheat straw and switchgrass, respectively. C is MA concentration in mol/L, and t is reaction time in min.

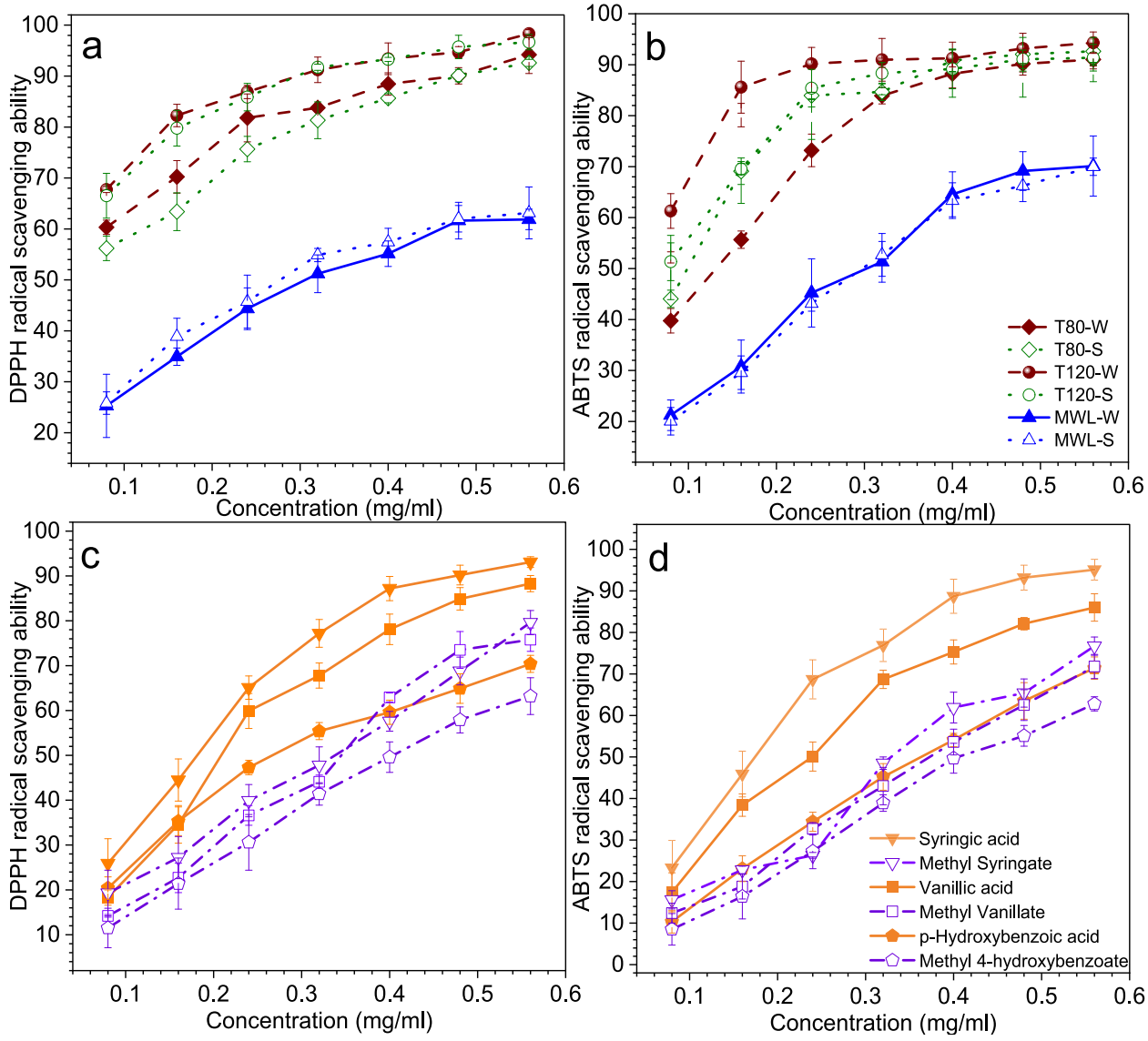

Fig. 3. Radical scavenging capability of MWLs and MAHLs (a, b) and lignin monomers (c, d) toward DPPH (a, c) and ABTS (b, d) radicals in a range of lignin concentrations from 0.08 to 0.56 mg/mL.

MWL was prepared using a classical method [29,30]. Air-dried wheat straw and switchgrass were milled to pass 30 mesh in a Wiley mill (Model No. 2, Thomas Scientific, Swedesboro, New Jersey, USA). Then, the dried powder was milled in a vibratory ball mill (PM100, Retsch, Haan, Germany) for 12 h.

2.3. Characterization of MAHLs and MWLs

Acetylated lignin was prepared according to previous work [24] for GPC analyses. Acetylated MAHLs were dissolved in tetrahydrofuran (THF, HPLC grade) with a concentration of 1 mg/mL and analyzed by gel permeation chromatography (GPC, LC-20 A, Shimadzu, Japan) using an organic size-exclusion chromatography column (KF-804, 300 mm × 8 mm i.d., 7 μm) calibrated with polystyrene standards (peak Mw of 1000, 2000, 3000, 10,000, and 40,000 g/mol). The column was heated at 40 °C and eluted with THF at 1 mL/min. All samples were freeze-dried before analyses.

2D $^{1}H—^{13}C$ heterogeneous single quantum correlation (HSQC) NMR lignin spectra were acquired using a Bruker (Billerica, Massachusetts, USA) AVANCE 500 MHz spectrometer. As described previously [24], 70 mg of lignin were dissolved in 0.5 mL of DMSO-d_6. Spectra were acquired using 40 scans and an interscan delay of 1 s for 3 h. A 12-ppm sweep was used. Topspin 3.5pl7 was used for the interactive integration of the cross peaks after the central DMSO solvent peak was referenced. Spectral images were colored using Adobe Illustrator CS6 (Adobe Systems, Inc., San Jose, California, USA). Chemical structures were drawn using ChemDraw Pro 14.0 (PerkinElmer, Waltham, Massachusetts, USA). ^{31}P NMR analyses were conducted at the Advanced Analysis and Testing Center of Nanjing Forestry University with a Bruker Ascend™ 600 MHz NMR spectrometer. 20 mg of nonacetylated lignin was dissolved in 0.5 mL anhydrous pyridine-d_5/$CDCl_3$ (1.6/1, *v*/v) solution. 100 μL of cyclohexanol (11.02 mg/mL, internal standard) and 100 μL chromium (III) acetylacetonate (5 mg/mL, relaxation regent), prepared using anhydrous pyridine-d_5/$CDCl_3$ solution were mixed with lignin solution and then added to 60 μL phosphorylating regent (2-chloro-4,4,5,5-tetramethyl-1,2,3-dioxaphospholane). After shaking for 30 min, the mixture was immediately analyzed.

2.4. Assay of antioxidant property

The antioxidant property of lignin samples was evaluated using DPPH and ABTS radical scavenging assays by a spectrophotometric

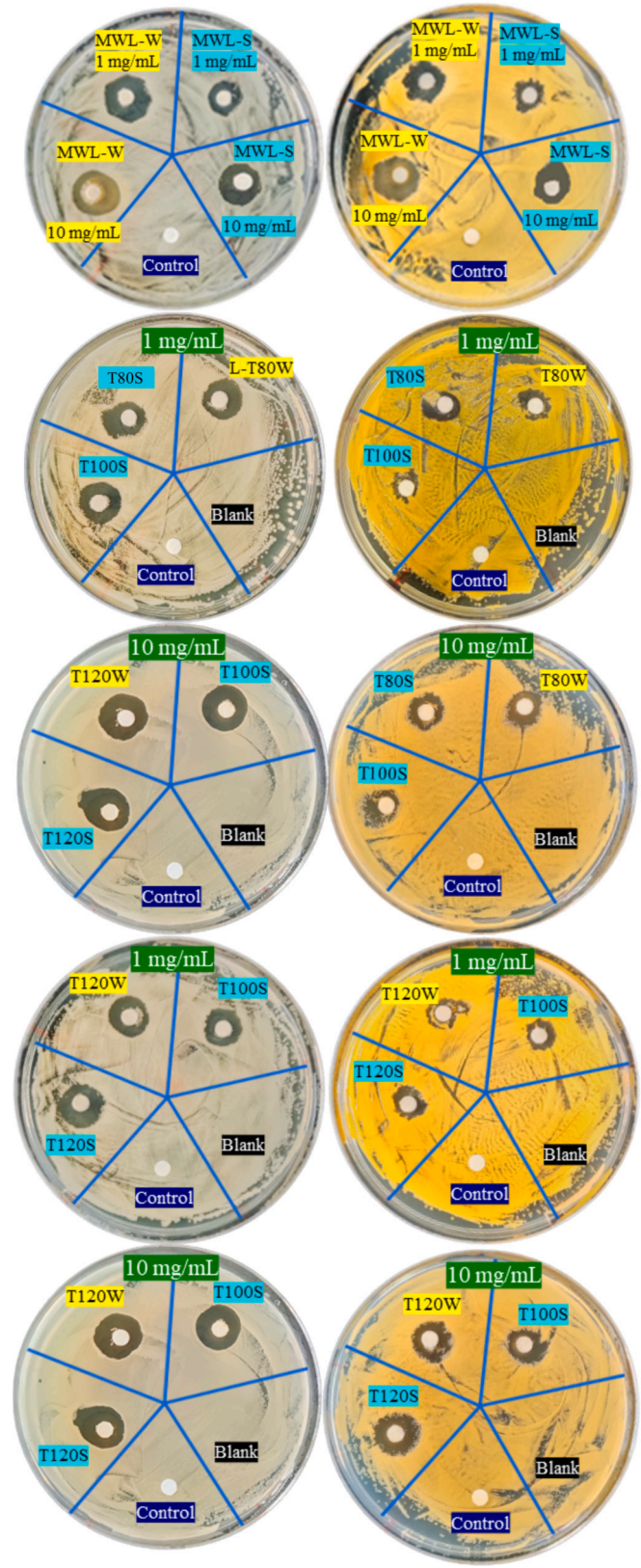

Fig. 4. Inhibition zones of *E. coli* (left column) and *S. aureus* (right column) by MAHLs as well as MWLs at 1 mg/mL and 10 mg/mL; White discs with yellow (wheat straw lignin) or cyan (switchgrass lignin) labels were added lignin solutions (dissolved in DMSO-ethanol) at different concentrations (tested samples). The gray rings around the white discs were inhibition zones. White discs with navy blue labels were controlled without lignin (only DMSO-ethanol solution). Blank simply shows the background color.

method according to previous studies [24,31,32]. Briefly, the lignin preparations (MAHLs and MWLs) were dissolved in dimethyl sulfoxide/water (9/1, *v*/v) at different concentrations (0.08–0.56 mg/mL), and then tested with DPPH and ABTS radical solution. The amounts of remaining DPPH and ABTS in the assays were analyzed by a spectrophotometer (Model 8453, Agilent Technologies, Palo Alto, California, USA) at 517 and 734 nm, respectively.

2.5. Determination of antibacterial property

The antibacterial activity of MAHLs and MWLs toward gram-positive *S. aureus* and gram-negative *E. coli* was assessed following the bacterial sensitivity filter-paper disc method [10]. The bacterial cultures were diluted with LB broth to an $OD_{600} = 0.5$. Briefly, a suspension of 48-h-old LB broth of the test bacterium (200 μL on each plate) was spread on the LB agar medium plates using a sterile glass spreader. Lignin has dissolved in DMSO-ethanol (4:1, *v*/v) solution at different bacterial concentrations of 1 to 10 mg/mL. Under aseptic conditions, empty sterilized discs (6 mm in diameter) were impregnated with 20 μL of a lignin solution and placed on the agar surface. A paper disc moistened with DMSO-ethanol solution was placed on the seeded Petri plate as vehicle control. The OD_{600} of bacterial suspensions was used as the control. The samples were incubated for 24 h at 37 °C. After the incubation period, the zone of inhibition diameter at each well was measured with a caliper and recorded. The antibacterial (*E. coli* or *S. aureus*) ability of the lignin was determined using Eq. (1) [33].

$$\text{Inhibition rate} = \frac{(D_T \quad D_C)}{D_T} \times 100\% \tag{1}$$

D_T is the diameter of the inhibition circle for the treatment group using the lignin solution, and D_C is the diameter of the inhibition circle for the control group.

2.6. Measurement of UV-blocking property

The UV-blocking performance of MAHLs and MWLs was measured by a near-infrared UV spectrophotometer (Lambda-950, PerkinElmer). Each lignin sample was dissolved in an aqueous dioxane solution (90 % *v*/v) at different concentrations in several quartz cuvettes. Each mixture was illuminated by the light source of the spectrometer. The transmittance (T) was measured in the wavelength range of 200–800 nm. The T_{UVA} (320–400 nm), T_{UVB} (280–320 nm), as well as T_{UV} (200–400 nm) of the MAHLs and MWLs were calculated using Eqs. (2)–(4), respectively [34]:

$$T_{UVA} = \frac{\int_{320}^{400} T_\lambda d\lambda}{\int_{320}^{400} d\lambda} \tag{2}$$

$$T_{UVB} = \frac{\int_{280}^{320} T_\lambda d\lambda}{\int_{280}^{320} d\lambda} \tag{3}$$

$$T_{UV} = \frac{\int_{200}^{400} T_\lambda d\lambda}{\int_{200}^{400} d\lambda} \tag{4}$$

where T_λ is spectral transmittance and λ is the wavelength. Then, the blocking percentages for UVA, UVB, and UV were calculated as follows (Eqs. (5)–(7)) [14]:

$$\text{UVA blocking} = 1 \quad T_{UVA} \tag{5}$$

$$\text{UVB blocking} = 1 \quad T_{UVB} \tag{6}$$

$$\text{UV blocking} = 1 \quad T_{UV} \tag{7}$$

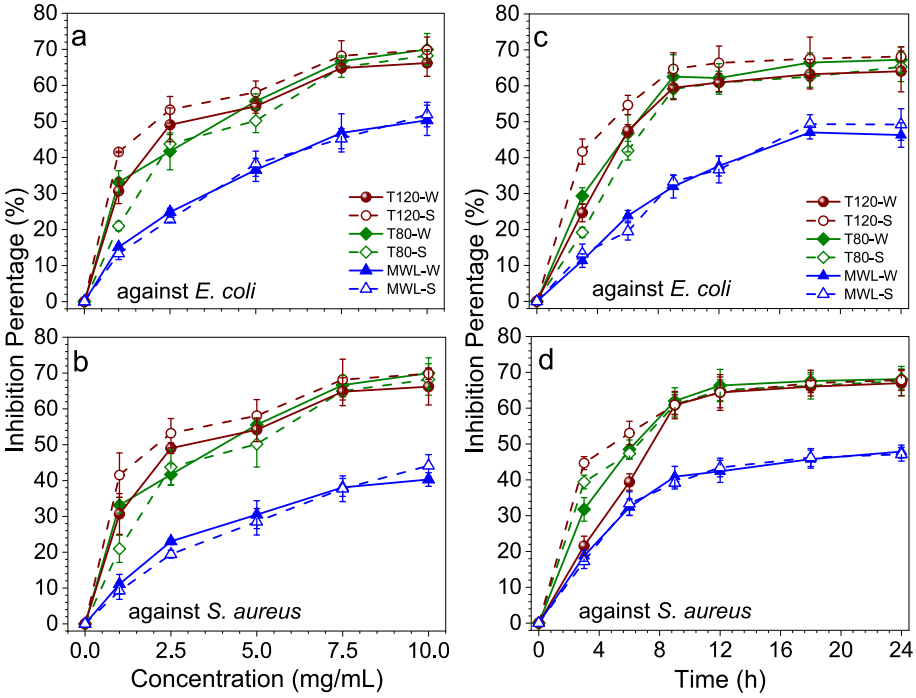

Fig. 5. Inhibition against (a) *E. coli* after 12 h and (b) *S. aureus* after 24 h by MAHLs and MWLs under different lignin concentrations; Inhibition rate curves (killing curves) of (c) *E. coli* and (d) *S. aureus* by MAHLs and MWLs at lignin concentration of 10 mg/mL.

2.7. Statistical analysis

Linear regression was used to analyze the relationships between the physicochemical structures with bioactivities. Best models were obtained based on adjusted R-squared values. Pearson correlations between the individual lignin properties and the bioactivities were calculated. All computations were performed using the R functions, and the regression model-selection process was performed using the Treg subsets function in the leaps R-package with the secret method selected. The heat map was rendered in Excel (Microsoft Corporation, Redmond, Washington, USA).

3. Results and discussion

3.1. Physical properties of MAHLs

Both the Mw and PDI of MAHLs were lower than their corresponding values of MWL from the same biomass and decreased with increasing fractionation severity, as shown in Fig. 1a. For MAHF at 80 °C, the Mw for both wheat straw and switchgrass were approximately 8000 compared with approximately 13,000 for MWL. PDI was approximately 2.0 or 30 % lower than the values of their corresponding MWLs.

The decrease in Mw resulted from lignin depolymerization by MAHF due to acid catalysis [20,24]. The lower PDI of MAHLs indicated narrower or more uniform molecular weight distributions (Fig. 1b), suggesting that the MAHLs mainly underwent depolymerization rather than repolymerization. With increasing severity, the Mw and PDI of MAHLs decreased as well. These results suggested that MAHF could produce uniform and low Mw lignin, which can enhance bioactivities [17].

3.2. ^{31}P NMR analysis

^{31}P NMR spectra of MWLs and MAHLs were used to determine the lignin -OH and -COOH contents [35]. As shown in Fig. 2a and b, MAHF resulted in a substantially lower aliphatic-OH content of 0.73 mmol/g for T120W compared with that of MWL-W of 3.09 mmol/g, suggesting that more aliphatic OH were substituted with increasing reaction severity [20]. -COOH group content increased from 0.43 mmol/g for T80W to 0.89 mmol/g for T120W. The same trend was also observed in MAHLs from switchgrass. The carboxylation of MAHLs by MA during the MAHF process was also confirmed by 2D NMR analysis. The content of phenolic-OH in MAHLs was also increased with increasing fractionation severity, indicating that many β-O-4′ linkages were cleaved during MAHF. No significant change in *p*-hydroxyl -OH was observed from all MAHLs as demethylation reactions were absent in the MAHF.

3.3. 2D HSQC NMR analysis

To understand the structure features of lignin, the MAHLs and MWLs were analyzed by 2D HSQC NMR spectroscopy (Fig. S1). Strong signals of the methoxy group, β-O-4′ linkage (A), phenyl coumarins (B), and resinols (C) can be observed in the side-chain regions of 2D HSQC spectra from all lignin preparations. Signals from carbohydrates can also be seen, such as β-D-xylopyranoside units (X), arabinofuranoside units (Ara), and 4-*O*-methyl-α-D-glucuronic acid units (U).

β-O-4′ linkages in T80W were 48.8 % lower than that in MWL-W (Table 2). The content of β-O-4′ linkages in MAHLs decreased with increasing fractionation severity. The β-O-4′ linkages in MAHL-W (wheat straw) from M60T120t30 were less than half of the amount found in MWL-W. The condensation degree of MAHL-W was greater than the corresponding value of MAHL-S (switchgrass) under the same fractionation condition and obviously increased with increasing fractionation severity. Similarly, β-β’ and β-5′ increased rapidly with increasing fractionation severity for both wheat straw and switchgrass, suggesting that MAHF could modify the chemical structures of MAHLs by controlling fractionation severity. MAHL-W has rich S unit lignin (high S/G ratio, Table 2). The S unit lignin cannot participate in the formation of C—C linkages at the 5-position. Therefore, its condensation structure was mainly formed at the β-position to result in high β-β’ contents. In the spectrum (Fig. S1), the strong cross-signals at δ_C/δ_H 128.5/6.23, 132.3/6.39, and 63.5/(3.83, 4.30) ppm were the evidence of lignin esterification (carboxylation) by MA at the γ-OH position to form E_γ(MA) [20]. The esterification of MAHLs increased with increasing MAHF severity, and the peak areas of $E_\gamma(MA)_{2,3}$ from T100-W at 128.5/6.23 and 132.3/

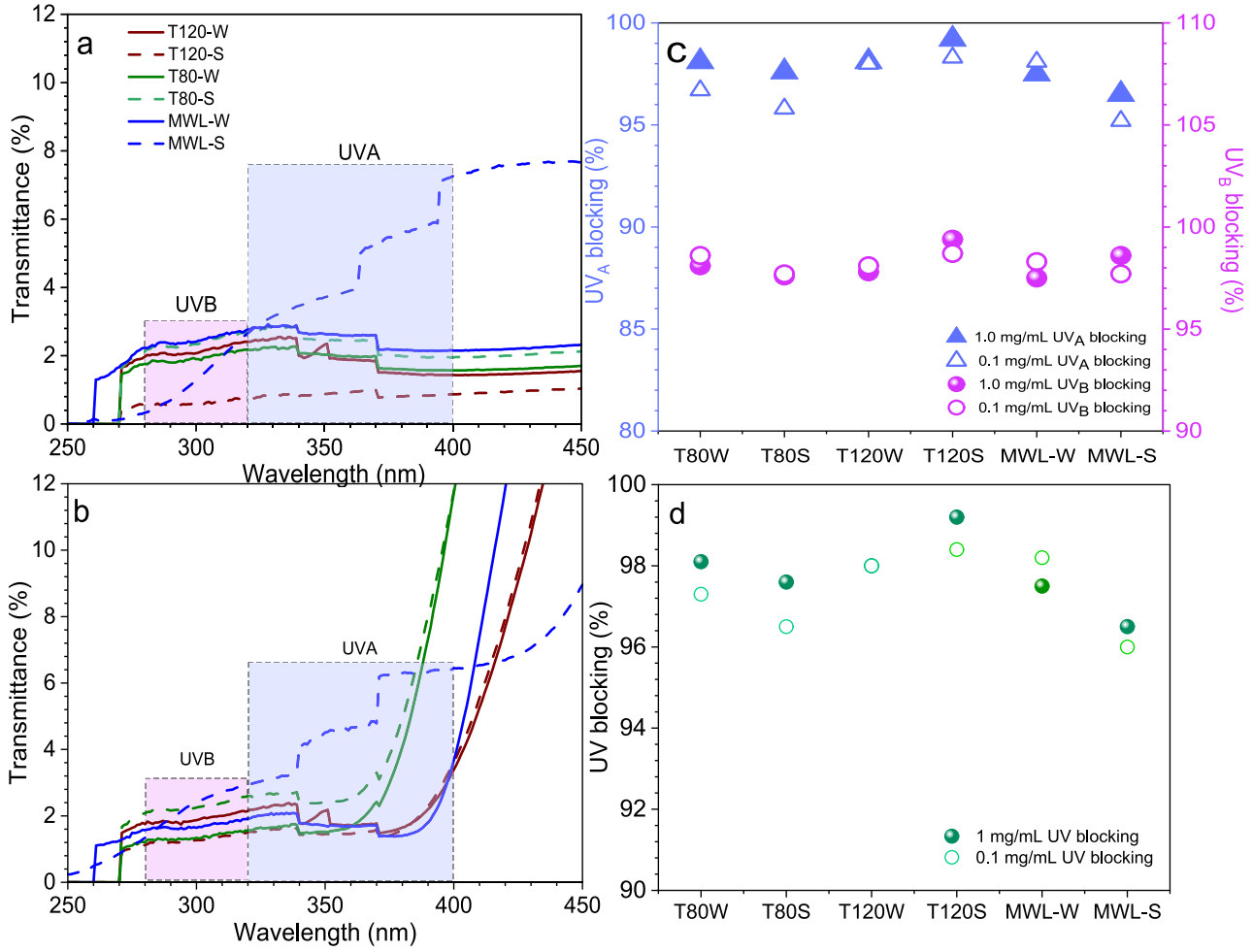

Fig. 6. UV–vis transmission spectra of MAHL and MWL solutions at (a) 1 mg/mL and (b) 0.1 mg/mL; UV blocking by MAHL and MWL solutions at 1 and 0.1 mg/mL by (c) UV_A and UV_B and (d) overall.

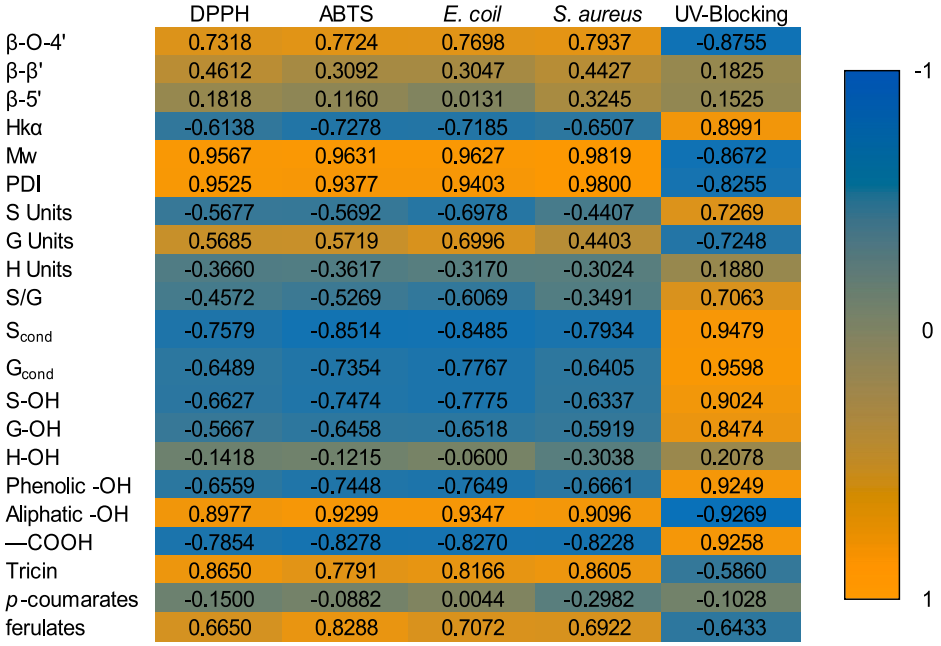

Fig. 7. The heat map of the Pearson correlation between lignin structural features and its biological activities. Orange represents a positive correlation (≥0.0), and blue represents a negative correlation (≤0.0). The darkness of color reflects the strength of the correlation.

Table 3
Linear regression model coefficients. Adjusted R-squared values are based on the eight observations detailed earlier in this section.

Response	DPPH	ABTS	*E. coli*	*S. aureus*	UV blocking
Intercept	0.18096	0.13428	17.672	8.335	62.594
β-O-4′	0.00959	0.00469			
Mw				0.001095	
PDI	0.22808	0.1193	7.753		
Aliphatic -OH	0.10136	0.0771			
Ferulates		0.0229			
Phenolic -OH			3.2456	2.948	
Tricin			0.1578		
p-coumarates			0.1995		
S/G					8.225
-COOH					27.376
Adj. R-Squared	0.9913	0.9946	0.9994	0.9966	0.9265

6.39 ppm were significantly increased compared with those from T80-W (Fig. S1). The signal intensities of $E_{\gamma}(MA)_{2,3}$ from T100-S were stronger than those of T100-W, consistent with the extent of γ-esterification as listed in Table 2 (i.e., 41 % vs. 28 %). With increasing fractionation severity, the S/G ratio of MAHL increased significantly, especially for MAHL-W, i.e., the S/G ratio of T120W was twice as much as that of MWL-W. The same was also observed in MAHL-S. This phenomenon is probably due to the more rapid decrease in G unit lignin signal with increasing severity than the decrease in S unit lignin signal. Other internal structures, e.g., LCC linkages or tricin, were also decreased with increasing fractionation severity.

3.4. Lignin antioxidant property

All MAHLs showed better antioxidant ability than their corresponding MWL toward both DPPH and ABTS free radicals. The reported data were averages of three replicate experiments. As shown in Fig. 3a, b, increasing lignin concentration increased radical scavenging ability. When lignin concentration was >0.4 mg/mL, the elimination curves for the two examined free radicals became stable. The MAHLs showed better antioxidant activities than the MWLs, i.e., at 0.56 mg/mL. T120S had almost 1.6 times the scavenging ability of the DPPH radicals. The MAHLs from severe fractionation conditions, e.g., T120W, exhibited greater antioxidant activities than those from mild fractionation conditions, e.g., T80W. These results indicated that MAHLs with higher phenolic -OH and -COOH contents obtained under more severe MAHF conditions exhibited greater antioxidant activity.

To assess which type of -OH in lignin provides significant antioxidant ability, lignin monomer model compounds including syringic acid (SA), methyl syringate (MS), vanillic acid (VA), methyl vanillate (MV), p-hydroxybenzoic acid (HA), and methyl 4-hydroxybenzoate (MH) were tested in a concentration range from 0.08 to 0.56 mg/mL. As shown in Fig. 3c, d, the lignin phenolic acids (SA, VA, and HA) showed greater antioxidant ability than the phenolic esters (MS, MV, and MH). This suggests that the carboxylic acid groups -COOH from MA esterification outperformed the ester group from the side chain of lignin for enhancing antioxidant activity. Furthermore, SA showed the highest antioxidant ability, suggesting S units of MAHLs played an important role in free radical scavenging. S units usually have two methoxy groups that can activate the aromatic ring of lignin through an electron-withdrawing-inducing effect to trap more radicals [36,37]. In comparison, G and H units carry one and zero methoxy groups, respectively, resulting in low lignin antioxidant activity [37], which suggests that lignin with higher S content or S/G ratio could have better antioxidant property.

3.5. Lignin antibacterial activity

The growth inhibition capacities of MAHLs and MWLs against the two selected bacteria (*E. coli* and *S. aureus*) were evaluated by agar diffusion as shown in Fig. 4. It was observed that the MAHLs and MWLs created a gray antibacterial ring around the bacterium culture (white disc), suggesting that these lignin samples had effective antibacterial property against the two microbes. However, the inhibition rings created by some lignin samples were not perfect circles, i.e., T80S or T120W against *S. aureus*. This phenomenon was probably due to the uneven diffusion of lignin in the liquid agar medium or the uneven growth of bacteria in the medium due to their motility and responses to environmental stresses, leading to variations in the antimicrobial activity of lignin in different directions and directional variations in inhibition rings.

Increasing the concentration of MAHL solution increased the area of the inhibition zones. The inhibition of *E. coli* increased from 32 % (calculated using Eq. (1)) by T120S at 1 mg/mL to 68 % at 10 mg/mL (Fig. 5a). Additionally, the areas of inhibition zones against *S. aureus* (right column in Fig. 4) were smaller than those against *E. coli* using the same lignin sample at the same loading. This indicates that MAHLs had stronger antimicrobial activity against gram-negative bacteria (*E. coli*) than against gram-positive ones (*S. aureus*). The difference in the antibacterial activity of MAHLs between gram-positive and gram-negative bacteria was perhaps due to the difference in the cell wall structure between the two bacteria [38].

The inhibition rate curves (with respect to time in 12 h), also called killing curves (Fig. 5 c, d), indicate that MAHL-S from switchgrass had similar antibacterial activity behavior to MAHL-W from wheat straw toward both microbes. T120S and T120W at a dosage of 10 mg/mL could kill >35 % of both bacteria within 12 h (Fig. 5c, d). The MAHLs from severe fractionation, i.e., T120S and T120W, had better antibacterial activities than those from mild fractionation runs. For example, the inhibition percentage against *E. coli* by T120S was 66 % compared with 56 % by T80S and 36 % by MWL-S in 12 h. This was due to the higher phenolic -OH and -COOH contents and lower Mw of T120S compared with those of T80S and MWL-S. The greater contents of phenolic -OH or -COOH of lignin could change the surrounding pH environment of bacteria, which decreases the mobility of microbes. Moreover, the lower Mw lignin had a greater ability to penetrate deeper into bacterial cell membranes compared with the higher Mw lignin [39].

3.6. Lignin UV-blocking activity

The UV-blocking properties of MAHLs and MWLs were evaluated by measuring their transmittance and absorption spectra in the UV–vis range from 200 to 800 nm. Compared with MWLs, MAHLs had greater abilities in blocking UV rays at all loadings as shown by the lower spectral transmittance in Fig. 6a, except for switchgrass MWLs at 1 mg/L loading in UV_B. Switchgrass MAHLs from severe fractionation, i.e., T120-S, exhibited greater abilities in blocking UV_A and UV_B than the corresponding MAHLs from mild fractionation (Fig. 6a, b), perhaps due to the greater content of functional groups (phenolic -OH, -COOH, and HKα), which could be conjugated with the benzene rings of lignin to shield or reflect UV light [4,6]. Moreover, by increasing the bio-functional group content, i.e., phenolic -OH and -COOH, the UV-blocking capacity was enhanced (Fig. 6d). For example, MWL-W with

1.3 mmol/g and T120W with 2.0 mmol/g phenolic -OH (Fig. 2b) blocked approximately 98 % of UV (Fig. 6c). It is understood that the proportion of UV_B in UV radiation is lower than that of UV_A. However, UV_B as a shorter wavelength radiation is more harmful in terms of potentially causing skin cancer than UV_A. Therefore, materials with outstanding UV_B-blocking ability are effective for skin cancer prevention.

All lignin preparations had an average transmittance in the UV_B range below 5 %, suggesting great shielding capacities against UV_B. Increasing lignin concentration did not improve UV_B-blocking performance as shown in Fig. 6c. At a low lignin solution of 0.1 mg/mL, however, UV_A blocking was significantly decreased especially at a wavelength >350 nm (Fig. 6a). Overall, MAHLs were proved to be effective as a natural remedy for blocking UV radiation from the sun.

3.7. Lignin structures-activity relationships

Multiple regression models and Pearson correlation, ρ, were utilized to assess the magnitudes and significance of these relationships, as shown in Fig. 7, Figs. S2, S3, and S4. A Pearson correlation with an absolute value greater than approximately 0.7 is statistically significant for these data. The internal lignin molecular linkages, i.e., β-O-4′, had a significant impact on biological activities (Fig. 7). The antioxidant, antibacterial, and UV-blocking properties of lignin increased as β-O-4′ linkages decreased. The -COOH and HKα (C═O bonds) were found to be closely related to the enhancement of UV-blocking properties. These results suggested that the introduction of -COOH or the formation of C═O and C═C bonds in lignin during MAHF played a significant role in stabilizing radicals and shielding against UV radiation through conjugation action between the double bonds and aromatic rings of lignin [40,41]. Moreover, the physical properties of lignin (Mw and PDI) were positively associated with the corresponding multiple bioactivities. Lignin with smaller and more uniform Mw exhibits great antioxidant or UV-blocking properties due to the easy stabilization of free radicals and shielding UV radiation [13].

Compared with the Pearson correlation of S and G unit lignin ($|\rho| > 0.7$, Fig. 7), the S_{cond} and G_{cond} unit lignin provided important contributions to the three biological activities, particularly for UV-blocking, with $|\rho| > 0.9$ (Fig. 7). Interestingly, no Pearson correlation values of the H units with diverse bioactivities were statistically significant ($|\rho| < 0.3$). These results suggested that -OCH_3 promoted the chemical activity of the benzene ring in lignin due to its electron-donating properties [42], which made the π electron density of the aromatic rings greater than that of the aromatic rings without -OCH_3. Furthermore, the side chain of S_{cond} and G_{cond} units contains C═C bonds, i.e., HKα or -COOH, and the aromatic rings with one or two -OCH_3. The presence of these groups can enhance the effects of S_{cond} and G_{cond} unit lignin p-π conjugation and thereby increase the ability of lignin to stabilize lignin and absorb UV light.

The bioactive structures that afforded the most bioactivity in lignin were the -OH groups [43,44]. It can be seen from Fig. 7 that the aliphatic -OH of S and G unit lignin had a strong negative correlation with all biological activities ($|\rho| > 0.9$, Fig. 7), perhaps because aliphatic -OH was located on the side chain, which cannot be ionized and increases acidity. This suggests that multiple bioactivities of lignin would be improved with decreasing aliphatic -OH. As shown in Fig. 2b, the phenolic -OH and -COOH content of MAHLs increased with increasing fractionation severity when the aliphatic -OH content was removed or oxidized during MAHF. As reported in previous works [36,45], phenolic -OH or -COOH could be ionized and conjugated with aromatic rings of lignin to form p-π conjugation systems, in which it was easy to stabilize the free radicals and block the UV. Furthermore, more phenolic -OH and -COOH of lignin could create a low pH environment around the bacterial cell membrane to disrupt the membrane proton motility [15,38], especially for a gram-negative bacterium such as *E. coli* ($|\rho| < 0.76$, Fig. 7). Becasue MAHF can substitute aliphatic -OH to result in increasing phenolic -OH and -COOH contet in MAHLs as revealed by ^{31}P NMR (Fig. 2), especially at increasing MAHL severities, MAHF has significnat advanatges for fractionate lignin with great bioactivities and UV-blocking properties.

Because some dependent variables shown in Fig. 7 are interdependent, for example, β-β', β-5′, S_{cond}, and G_{cond}, all are measures of the extent of lignin condensation and all are correlated to β-O-4′. Table 3 provides linear regression models for the five response variables. Although other models exist, these tend to exhibit the most reasonable prediction of biological activities.

4. Conclusion

This study successfully demonstrated that maleic acid hydrotropic fractionation (MAHF) extracted bioactive lignin with diverse physicochemical structure from two types of herbaceous biomass. The study offers a novel pathway to fractionate lignin with aliphatic -OH being substituted to result in increasing phenolic -OH and -COOH content, therefore with great bioactivities and UV-blocking properties. Furthermore, lignin structural diversity can be tailored by controlling fractionation severity. The study elucidated the relationship between the lignin structural characteristics and its antioxidant, antibacterial, and UV-blocking abilities. The results demonstrated that lignin with higher phenolic -OH, -COOH, and S/G ratios as well as lower molecular weights and polydispersity indices exhibited enhanced antioxidant and antibacterial properties and superior UV-blocking capabilities. Multivariate regression models and Pearson correlation analyses substantiated the significant influence of internal linkages, -COOH, and HKα on the bioactivity of lignin. Through linear regression, predictive linear models were developed to determine lignin bioactivities based on key independent variables. The findings from this study can advance the application of lignin in industries such as food, cosmetics, and pharmaceuticals, contributing to the goals of sustainable development and a low-carbon economy.

CRediT authorship contribution statement

Chen Su: Writing – original draft, Investigation, Conceptualization. **Xiu Wang:** Validation, Software. **Kolby Hirth:** Visualization, Data curation. **Matthew Arvanitis:** Writing – review & editing, Formal analysis. **Yunfeng Cao:** Supervision, Investigation, Funding acquisition. **Guigan Fang:** Supervision, Investigation, Funding acquisition. **J.Y. Zhu:** Writing – review & editing, Supervision, Resources, Conceptualization.

Declaration of competing interest

The authors declare that the correspomnding author JYZ is an inventor of a US patentn on Maleci acid hydrotropic fractionation. There are no competing interest for the rest of the authors.

Acknowledgments

This work was conducted while Chen Su was a visiting student at the USDA Forest Service, Forest Products Laboratory. The authors are grateful for financial support from the Key Laboratory of Biomass Energy and Material, Jiangsu Province (JSBEM-S-202316), National Natural Science Foundation of China (No. 22308373), Taishan Industry Experts Program (tscy20200213), and Special Fund for Basic Scientific Research Business of Central Public Research Institutes of China (No. CAFYBB2021ZI001-01). We also would like to acknowledge Fred Matt for conducting carbohydrate analyses, Rolland Gleisner for preparing switchgrass and wheat straw, and Prof. Kevin Shinner, Dept. of Biological Systems Engineering at the University of Wisconsin-Madison, for providing the switchgrass. The findings and conclusions in this study are those of the authors and should not be construed to represent any official

USDA or U.S. government determination or policy.

Appendix A. Supplementary data

Supplementary data to this article can be found online at https://doi.org/10.1016/j.ijbiomac.2025.140519.

Data availability

Data will be made available on request.

References

[1] J. He, Z. Li, X. Zhang, H. Wang, W. Dong, E. Du, S. Chang, X. Ou, S. Guo, Z. Tian, Towards carbon neutrality: a study on China's long-term low-carbon transition pathways and strategies, Environmental Science and Ecotechnology 9 (2022) 100134.

[2] C. Kennedy, N. Ibrahim, D. Hoornweg, Low-carbon infrastructure strategies for cities, Nat. Clim. Chang. 4 (5) (2014) 343–346.

[3] Z. Zhang, G. Hu, X. Mu, L. Kong, From low carbon to carbon neutrality: a bibliometric analysis of the status, evolution and development trend, J. Environ. Manage. 322 (2022) 116087.

[4] W.D.H. Schneider, A.J.P. Dillon, M. Camassola, Lignin nanoparticles enter the scene: a promising versatile green tool for multiple applications, Biotechnol. Adv. 47 (2021) 107685.

[5] A.D.E.S. Pereira, J. Luiz de Oliveira, S. Maira Savassa, C. Barbara Rogério, G. Araujo de Medeiros, L.F. Fraceto, Lignin nanoparticles: new insights for a sustainable agriculture, J. Clean. Prod. 345 (2022) 131145, https://doi.org/10.1016/j.jclepro.2022.131145.

[6] D. Kai, M.J. Tan, P.L. Chee, Y.K. Chua, Y.L. Yap, X.J. Loh, Towards lignin-based functional materials in a sustainable world, Green Chem. 18 (5) (2016) 1175–1200.

[7] I. Ullah, Z. Chen, Y. Xie, S.S. Khan, S. Singh, C. Yu, G. Cheng, Recent advances in biological activities of lignin and emerging biomedical applications: a short review, Int. J. Biol. Macromol. 208 (2022) 819–832.

[8] F. Shu, B. Jiang, Y. Yuan, M. Li, W. Wu, Y. Jin, H. Xiao, Biological activities and emerging roles of lignin and lignin-based products— a review, Biomacromolecules 22 (12) (2021) 4905–4918.

[9] R. Liu, L. Dai, C. Xu, K. Wang, C. Zheng, C. Si, Lignin-based micro-and nanomaterials and their composites in biomedical applications, ChemSusChem 13 (17) (2020) 4266–4283.

[10] G. Wang, T. Pang, Y. Xia, X. Liu, S. Li, A.M. Parvez, F. Kong, C. Si, Subdivision of bamboo Kraft lignin by one-step ethanol fractionation to enhance its water-solubility and antibacterial performance, Int. J. Biol. Macromol. 133 (2019) 156–164.

[11] A.G. Morena, A. Bassegoda, M. Natan, G. Jacobi, E. Banin, T. Tzanov, Antibacterial properties and mechanisms of action of sonoenzymatically synthesized lignin-based nanoparticles, ACS Appl. Mater. Interfaces 14 (33) (2022) 37270–37279.

[12] M. Lin, L. Yang, H. Zhang, Y. Xia, Y. He, W. Lan, J. Ren, F. Yue, F. Lu, Revealing the structure-activity relationship between lignin and anti-UV radiation, Ind. Crop. Prod. 174 (2021).

[13] H. Sadeghifar, A. Ragauskas, Lignin as a UV light blocker—a review, Polymers 12 (5) (2020) 1134.

[14] Y. Zhang, M. Naebe, Lignin: a review on structure, properties, and applications as a light-colored UV absorber, ACS Sustainable Chemistry & Engineering 9 (4) (2021) 1427–1442.

[15] Y.H. Xu, P. Zeng, M.F. Li, J. Bian, F. Peng, γ-Valerolactone/water system for lignin fractionation to enhance antibacterial and antioxidant capacities, Sep. Purif. Technol. 279 (2021) 119780, https://doi.org/10.1016/j.seppur.2021.119780.

[16] P.P. Akhila, K.V. Sunooj, S.P. Bangar, B. Aaliya, M. Navaf, B. Indumathy, S. Yugeswaran, S.K. Sinha, S.A. Mir, S. Mounir, J. George, M.-R. Nemțanu, Assessing the impact of plasma-activated water-assisted heat-moisture treatment on the extrusion-recrystallization process of hausa potato starch, Carbohydr. Polym. 335 (2024).

[17] C. Su, X. Wang, Y. Deng, T. Wu, J. Jiao, C. Huang, Y. Cao, H. Dai, G. Fang, Revitalizing multiple bioactivities of the lignin-carbohydrate complex through a two-step strategy: unraveling the enhancement origin from a structural variation perspective, ACS Sustainable Chemistry & Engineering 12 (28) (2024) 10544–10554.

[18] L. Zheng, G. Lu, W. Pei, W. Yan, Y. Li, L. Zhang, C. Huang, Q. Jiang, Understanding the relationship between the structural properties of lignin and their biological activities, Int. J. Biol. Macromol. 190 (2021) 291–300.

[19] R. Rinaldi, R. Jastrzebski, M.T. Clough, J. Ralph, M. Kennema, P.C. Bruijnincx, B. M. Weckhuysen, Paving the way for lignin valorisation: recent advances in bioengineering, biorefining and catalysis, Angew. Chem. Int. Ed. 55 (29) (2016) 8164–8215.

[20] C. Cai, K. Hirth, R. Gleisner, H. Lou, X. Qiu, J.Y. Zhu, Maleic acid as a dicarboxylic acid hydrotrope for sustainable fractionation of wood at atmospheric pressure and ≤ 100 °C: mode and utility of lignin esterification, Green Chem. 22 (5) (2020) 1605–1617, https://doi.org/10.1039/C9GC04267A.

[21] S. Jeong, J. Ryu, Q. Yang, J.Y. Zhu, C.G. Yoo, Recent advances in hydrotropic solvent systems for lignocellulosic biomass utilization, Green Chem. 26 (4) (2023) 1806–1830.

[22] J.Y. Zhu, L.H. Chen, C. Cai, Acid hydrotropic fractionation of lignocelluloses for sustainable biorefinery: advantages, opportunities, and research needs, ChemSusChem 14 (15) (2021) 3031–3046, https://doi.org/10.1002/cssc.202100915.

[23] C. Cai, J. Li, K. Hirth, G.W. Huber, H. Lou, J.Y. Zhu, Comparison of two acid hydrotropes for sustainabl fractionation of birch wood, ChemSusChem 13 (2020) 4649–4659, https://doi.org/10.1002/cssc.202001120.

[24] C. Su, K. Hirth, Z. Liu, Y. Cao, J.Y. Zhu, Acid hydrotropic fractionation of switchgrass at atmospheric pressure using maleic acid in comparison with p-TsOH: advantages of lignin esterification, Industrial Crops and Products 159 (2021) 13017, https://doi.org/10.1016/j.indcrop.2020.113017.

[25] J.Y. Zhu, U.P. Agarwal, P.N. Ciesielski, M.E. Himmel, R. Gao, Y. Deng, M. Morits, M. Österberg, Towards sustainable production and utilization of plant-biomass-based nanomaterials: a review and analysis of recent developments, Biotechnol. Biofuels 14 (2021) 114, https://doi.org/10.1186/s13068-021-01963-5.

[26] J. Zhu, N. Jiao, J. Cheng, H. Zhang, G. Xu, Y. Xu, J. Zhu, Integrated process for the co-production of bioethanol, furfural, and lignin nanoparticles from birch wood via acid hydrotropic fractionation, Renew. Energy 204 (2023) 176–184.

[27] Q. Ma, J. Zhu, R. Gleisner, R. Yang, J.Y. Zhu, Valorization of wheat straw using a recyclable hydrotrope at low temperatures (≤90 °C), ACS Sustain. Chem. Eng. 6 (2018) 14480–14489, https://doi.org/10.1021/acssuschemeng.8b03135.

[28] X. Luo, R. Gleisner, S. Tian, J. Negron, W. Zhu, E. Horn, X. Pan, J. Zhu, Evaluation of mountain beetle-infested lodgepole pine for cellulosic ethanol production by sulfite pretreatment to overcome recalcitrance of lignocellulose, Ind. Eng. Chem. Res. 49 (17) (2010) 8258–8266.

[29] M.Y. Balakshin, E.A. Capanema, H.-M. Chang, MWL fraction with a high concentration of lignin-carbohydrate linkages: isolation and 2D NMR spectroscopic analysis, Holzforschung 61 (1) (2007) 1–7.

[30] E. Capanema, M. Balakshin, R. Katahira, H.-M. Chang, H. Jameel, How well do MWL and CEL preparations represent the whole hardwood lignin? J. Wood Chem. Technol. 35 (1) (2014) 17–26.

[31] B. Jiang, Y. Zhang, L. Gu, W. Wu, H. Zhao, Y. Jin, Structural elucidation and antioxidant activity of lignin isolated from rice straw and alkalioxygen black liquor, Int. J. Biol. Macromol. 116 (2018) 513–519.

[32] Y.-M. Wang, X.-Y. Li, J. Wang, Y. He, C.-F. Chi, B. Wang, Antioxidant peptides from protein hydrolysate of skipjack tuna milt: purification, identification, and cytoprotection on H2O2 damaged human umbilical vein endothelial cells, Process Biochem. 113 (2022) 258–269, https://doi.org/10.1016/j.procbio.2022.01.008.

[33] A.G. Morena, A. Bassegoda, J. Hoyo, T. Tzanov, Hybrid tellurium-lignin nanoparticles with enhanced antibacterial properties, ACS Appl. Mater. Interfaces 13 (13) (2021) 14885–14893.

[34] H. Bian, L. Chen, M. Dong, L. Wang, R. Wang, X. Zhou, C. Wu, X. Wang, X. Ji, H. Dai, Natural lignocellulosic nanofibril film with excellent ultraviolet blocking performance and robust environment resistance, Int. J. Biol. Macromol. 166 (2021) 1578–1585.

[35] A. Granata, D.S. Argyropoulos, 2-Chloro-4, 4, 5, 5-tetramethyl-1, 3, 2-dioxaphospholane, a reagent for the accurate determination of the uncondensed and condensed phenolic moieties in lignins, J. Agric. Food Chem. 43 (6) (1995) 1538–1544.

[36] T. Dizhbite, G. Telysheva, V. Jurkjane, U. Viesturs, Characterization of the radical scavenging activity of lignins–natural antioxidants, Bioresour. Technol. 95 (3) (2004) 309–317.

[37] B. Jiang, Y. Zhang, H. Zhao, T. Guo, W. Wu, Y. Jin, Structure-antioxidant activity relationship of active oxygen catalytic lignin and lignin-carbohydrate complex, Int. J. Biol. Macromol. 139 (2019) 21–29.

[38] S. Shankar, J.-W. Rhim, K. Won, Preparation of poly (lactide)/lignin/silver nanoparticles composite films with UV light barrier and antibacterial properties, Int. J. Biol. Macromol. 107 (2018) 1724–1731.

[39] X. Dong, M. Dong, Y. Lu, A. Turley, T. Jin, C. Wu, Antimicrobial and antioxidant activities of lignin from residue of corn Stover to ethanol production, Industrial Crops and Products 34 (3) (2011) 1629–1634.

[40] O.B. Diógenes, D.R. de Oliveira, L.R. da Silva, Í.G. Pereira, S.E. Mazzetto, W. S. Araujo, D. Lomonaco, Development of coal tar-free coatings: acetylated lignin as a bio-additive for anticorrosive and UV-blocking epoxy resins, Prog. Org. Coat. 161 (2021) 106533.

[41] M.H. Tran, D.-P. Phan, E.Y. Lee, Review on lignin modifications toward natural UV protection ingredient for lignin-based sunscreens, Green Chem. 23 (13) (2021) 4633–4646.

[42] X. Ren, P. Wang, X. Han, G. Zhang, J. Gu, C. Ding, X. Zheng, F. Cao, Depolymerization of lignin to aromatics by selectively oxidizing cleavage of C–C and C–O bonds using CuCl2/polybenzoxazine catalysts at room temperature, ACS Sustain. Chem. Eng. 5 (8) (2017) 6548–6556.

[43] X.-C. Cheng, X.-R. Guo, Z. Qin, X.-D. Wang, H.-M. Liu, Y.-L. Liu, Structural features and antioxidant activities of Chinese quince (Chaenomeles sinensis) fruits lignin during auto-catalyzed ethanol organosolv pretreatment, Int. J. Biol. Macromol. 164 (2020) 4348–4358.

[44] C. Su, T. Gan, Z. Liu, Y. Chen, Q. Zhou, J. Xia, Y. Cao, Enhancement of the antioxidant abilities of lignin and lignin-carbohydrate complex from wheat straw by moderate depolymerization via LiCl/DMSO solvent catalysis, Int. J. Biol. Macromol. 184 (2021) 369–379.

[45] L. Yao, L. Xiong, C.G. Yoo, C. Dong, X. Meng, J. Dai, A.J. Ragauskas, C. Yang, J. Yu, H. Yang, X. Chen, Correlations of the physicochemical properties of organosolv lignins from Broussonetia papyrifera with their antioxidant activities, Sustainable Energy Fuels 4 (10) (2020) 5114–5119.